A mechanically coupled reaction diffusion model of breast tumor response during neoadjuvant chemotherapy

Jared A. Weis[a,b], Michael I. Miga[a-d], Xia Li[a], Lori R. Arlinghaus[a], A. Bapsi Chakravarthy[e,f], Vandana Abramson[f,g], Richard G. Abramson[a,b,f], Jaime Farley[f,g], Thomas E. Yankeelov[a-c,f,h,i]
[a]Vanderbilt University Institute of Imaging Science, [b]Departments of Radiology and Radiological Sciences, [c]Biomedical Engineering, [d]Neurosurgery, [e]Radiation Oncology, [f]Vanderbilt-Ingram Cancer Center, [g]Medical Oncology, [h]Physics and Astronomy, [i]Cancer Biology, Vanderbilt University, Nashville, TN

ABSTRACT

There is currently a paucity of reliable techniques for predicting the response of breast tumors to neoadjuvant chemotherapy. The standard approach is to monitor gross changes in tumor size as measured by physical exam and/or conventional imaging, but these methods generally do not show whether a tumor is responding until the patient has completed therapy. One promising approach to address this clinical need is to integrate quantitative *in vivo* imaging data into biomathematical models of tumor growth in order to predict eventual response based on early measurements during therapy. Contrast enhanced and diffusion weighted magnetic resonance imaging data acquired before and after the first cycle of therapy to calibrate a patient-specific response model can be used to predict patient outcome at the conclusion of therapy. We have developed a mathematical modeling approach to optimize key model parameters for the calibration of a patient-specific mechanically coupled reaction-diffusion model of response. We apply the approach to patient data in which tumors were either responsive or non-responsive to neoajuvant chemotherapy and demonstrate changes to the patient-specific model which result in altered growth patterns. Additionally, we show that reconstructed parameter maps exhibit drastic differences between patients with different tumor burden outcomes at the conclusion of therapy, in this case, a 10-fold increase in proliferative capacity is found for a non-responding tumor versus its responsive counterpart. Finally, we show that the mechanically coupled reaction-diffusion growth model, when projected forward, more accurately predicts residual tumor burden than the uncoupled model.

Keywords: tumor growth, breast cancer, mathematical model, neoadjuvant chemotherapy, reaction-diffusion model, parameter reconstruction, mechanical model

1. INTRODUCTION

In the neoadjuvant setting, breast cancer patients receive therapy to reduce tumor size to allow more patients to undergo breast conservation therapy. Neoadjuvant therapy also provides an excellent opportunity to observe tumor sensitivity to a particular regimen. If we can predict early on in a patient's treatment that the treatment regimen is not effective, the treatment could be changed to another, potentially more effective regimen thereby avoiding unnecessary treatment related side effects and toxicities. With numerous therapy options now available, development of a method to predict response early in the course of neoadjuvant therapy is highly significant. This is especially relevant as targeted therapies are frequently cytostatic rather than cytotoxic and therefore the reliance on simple changes in tumor size is less useful. Unfortunately, evaluation of neoadjuvant therapy effectiveness by conventional means currently requires a long period of clinical observation, at the risk of letting unresponsive tumors become not resectable. Currently, the response of breast tumors to neoadjuvant therapy is monitored by gross changes in tumor size as measured by physical exam, conventional (i.e., morphological) magnetic resonance imaging (MRI), and/or ultrasound. Unfortunately, these methods generally do not show whether a tumor is responding until the patient has received several treatment cycles. New methods are needed to guide therapeutic interventions in this setting.

One promising approach to address this clinical need is to integrate the quantitative data available from emerging imaging modalities into physically realistic biomathematical models of tumor growth [1-4]. While some conditions can be diagnosed and monitored through conventional imaging, it is clear that conventional imaging alone is often insufficient to characterize therapeutic responses [5, 6]. The combination of quantitative data provided by advanced

medical imaging approaches to initialize and guide a mechanistic understanding provided by mathematical models may be a compelling strategy for these complex evaluations.

In this work, we use a mechanically coupled reaction diffusion tumor growth model coupled to the surrounding tissue stiffness to model and predict tumor response to neoadjuvant therapy. Estimation of tumor growth parameters within the model are driven by differences in tumor cell distributions measured early in the course of therapy (i.e., before and after one cycle of neoadjuvant therapy). Using the model, we then predict the tumor burden at the conclusion of neoadjuvant therapy and compare to experimental observations.

2. METHODS

2.1 Patient description

Patients who were undergoing neoadjuvant therapy as a component of their clinical care were eligible for the study. Further inclusion criteria included: 1) no previous systemic therapies for breast cancer, and 2) histologically documented invasive carcinoma of the breast with a sufficient risk of recurrence based on pre-treatment clinical parameters of size, grade, age, and nodal status to warrant the use of neoadjuvant therapy. Participating patients provided informed written consent to an Institutional Review Board approved study. The initial retrospective study described below compared modeling results from two patients: one "responsive" patient exhibiting complete pathological response (defined as no residual viable tumor on histologic analysis in breast or nodes at the completion of therapy) and one "non-responsive" patient exhibiting partial pathological response (defined as any residual invasive tumor on histologic analysis in breast or nodes at the completion of therapy).

2.2 MRI data acquisition

MRI was performed using a Philips 3T Achieva MR scanner (Philips Healthcare, Best, The Netherlands). THRIVE (T_1 High Resolution Isotropic Volume Examination) structural data was acquired *via* a 400×400×129 acquisition matrix over a 20 cm × 20 cm × 12.9 cm transverse field of view (FOV) with one signal acquisition, and TR/TE/α = 6.43 ms/3.4 ms/10^o. Dynamic contrast enhanced imaging (DCE-MRI) was acquired with an acquisition matrix of 192×192×20 (full-breast) over a sagittal square field of view (22 cm^2) with slice thickness of 5 mm, one signal acquisition, $TR/TE/\alpha$ = 7.9 ms/1.3 ms/20°, and a SENSE factor of 2. Each 20-slice set was at 25 time points. A catheter placed within an antecubital vein delivered 0.1 mmol/kg (9 – 15 mL, depending on patient weight) of the contrast agent gadopentetate dimeglumine, Gd-DTPA, (Magnevist, Wayne, NJ) at 2 mL/sec (followed by a saline flush) *via* a power injector (Medrad, Warrendale, PA) after the acquisition of three baseline dynamic scans.

Diffusion weighted MR imaging (DW-MRI) was acquired with a single-shot spin echo (SE) echo planar imaging (EPI) sequence in three orthogonal diffusion encoding directions, with b-values of 0 and 600 s/mm^2, FOV = 192×192 (uni-lateral), and an acquisition matrix of 96×96 reconstructed to 144x144. SENSE parallel imaging (acceleration factor = 2) and spectrally-selective adiabatic inversion recovery (SPAIR) fat saturation were implemented to reduce image artifacts. Subjects were breathing freely with no gating applied. The patient DW-MRIs consisted of 12 sagittal slices with slice thickness = 5 mm (no slice gap), TR = 3080 ms, TE = 'shortest' (41 or 60 ms), Δ = 19.8 or 29 ms, and δ = 10.7 or 21 ms, respectively, NSA = 10.

2.3 MRI data analysis

DCE-MRI, DWI-MRI, and anatomical T_1-weighted MR images were acquired at three time points: prior to beginning neoadjuvant therapy (initial), after one cycle of neoadjuvant therapy (post one cycle), and at the conclusion of 8-12 cycles of neoadjuvant therapy (final). Critical to the modeling approach is that all MR images for each patient are longitudinally coregistered across all time points. Therefore, the DCE-MRI scans from the initial and post one cycle time points were non-rigidly registered to the final time point using an adaptive basis algorithm with a tumor volume preserving constraint [7, 8]. As the DCE-MRI, DWI-MRI, and structural MRI were collected at the same time with minimal patient motion for each time point, the image sets can be readily longitudinally coregistered for each patient.

Following registration, DCE-MRI data sets at each time point were used to define a tumor region-of-interest (ROI) by comparing the averages of the baseline pre-contrast images and the enhanced post-contrast images. The tumor ROI was manually outlined on the difference image between the enhanced and the baseline images. Voxels in the manually drawn

ROI exhibiting 100% signal intensity increase between the average before and average after contrast infusion data were used to define the tumor voxels.

The diffusion data sets were fit to Eq. (1) to return apparent diffusion coefficient (ADC) values on a voxel-by-voxel basis:

$$ADC = \frac{\sum_{i=x,y,z} \ln(S_0/S_i)/b_i}{3} \quad (1)$$

where i is the diffusion-weighting direction, S_0 denotes the signal intensity in the absence of diffusion gradients, b reflects the strength and duration of a diffusion-sensitizing gradient, and S_i is the signal intensity in the presence of the diffusion-sensitizing gradient. Using Eq. (2), the ADC data for the tumor voxels (as defined by the DCE-MRI) was transformed to an estimate of tumor cell number, as described in [9],

$$N(\bar{x},t) = \theta\left(\frac{ADC_w - ADC(\bar{x},t)}{ADC_w - ADC_{\min}}\right) \quad (2)$$

where θ is the carrying capacity (i.e., the total number of tumor cells that fit within a voxel), ADC_w is the ADC of free water at 37° C (3×10^{-3} mm^2/s), $ADC(\bar{x},t)$ is the ADC value at position (x,y) in image space, and ADC_{min} is the minimum ADC value which corresponds to the voxel with the largest number of cells. To calculate θ, we assumed spherical tumor cells with a sphere packing density of 0.7405 [10]. We assumed a nominal tumor cell radius of 10 μm to arrive at a tumor cell volume of 4189 μm^2; from this value, and the voxel volume, the maximum number of tumor cells can be determined for a given voxel.

2.4 Mathematical modeling approach

The coupled set of PDE's governing the model are shown in Eqs. (3) - (5).

$$\frac{\partial N(\bar{x},t)}{\partial t} = \nabla\cdot\left(D\nabla N(\bar{x},t)\right) + k(\bar{x})N(\bar{x},t)\left(1 - \frac{N(\bar{x},t)}{\theta}\right) \quad (3)$$

$$D = D_o e^{-\gamma\sigma_{vm}(\bar{x},t)} \quad (4)$$

$$\nabla\cdot\sigma + \lambda\nabla N(\bar{x},t) = 0 \quad (5)$$

Eq. (3) models the rate of change of tumor cell number at a particular location and time as the sum of random cell diffusion (the first term on the right hand side of the equation) and logistic growth (the second term). The cell diffusion term is linked to surrounding tissue stiffness *via* Eq. (4), where σ_{vm} is defined as von Mises stress and γ is an empirically derived coupling constant. Eq. (5) describes mechanical equilibrium and governs how the stress tensor is subject to an expansive force determined by changes in tumor cell number ($N_{TC}(\bar{x},t)$) and a coupling constant λ. In this work, we model the mechanics by a 2-D linear-elastic, isotropic constitutive relation under the plane strain approximation.

Figure 1 shows the modeling approach for characterizing tumor cell growth and migration by mechanically coupling a reaction-diffusion tumor growth model to the surrounding tissue properties. A Levenberg-Marquardt least squares non-linear optimization was used to fit the spatially varying proliferation rate and global tumor cell diffusion term ($k(\bar{x},t)$ and D_0, respectively) between the tumor cell numbers at the initial and post one cycle time points. Note that $k(\bar{x},t)$ can have positive or negative values, describing either proliferation or cell death. The central slice 2-D coupled forward model is solved for tumor cell number and displacement by a fully explicit, finite difference in time domain, finite element simulation. Implicit within each time step of the forward tumor growth model is a calculation of von Mises stress, which is based on the displacement governed by changes in tumor cell number. Following optimization between the first two time points, the $k(\bar{x},t)$ and D_0 parameters were fixed and the model was projected forward in time in order to predict tumor cellularity at the final time point and was compared to observations.

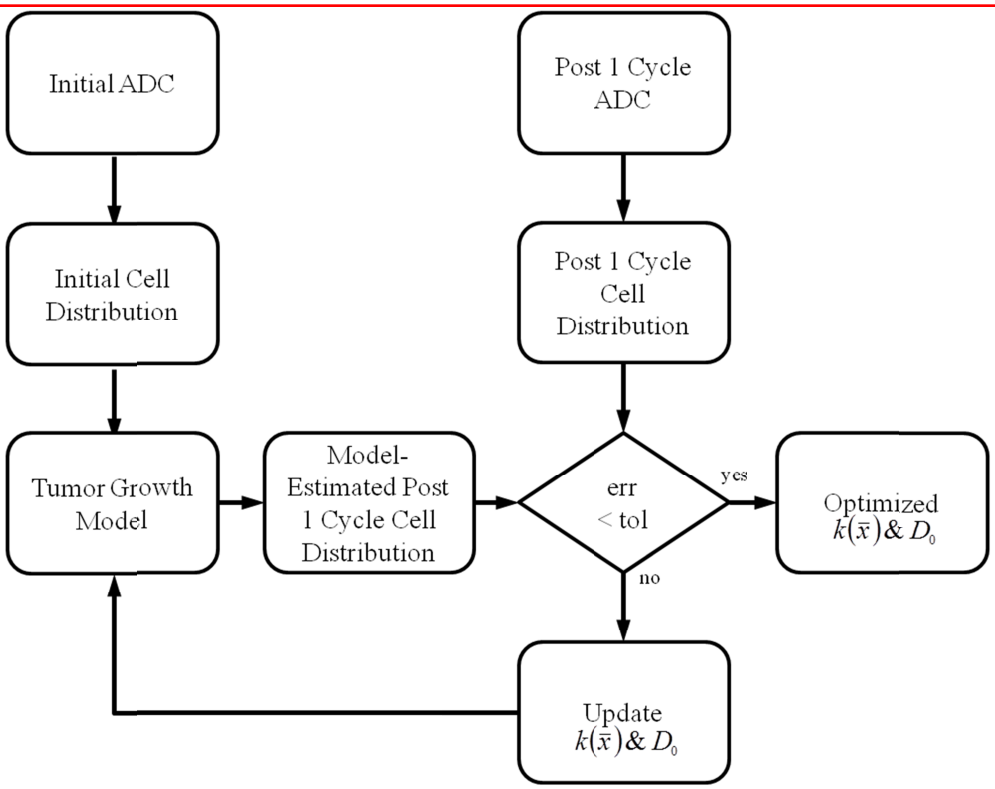

Figure 1. Inverse modeling approach for characterizing tumor cell growth parameters. The initial and post one cycle ADC maps of the tumor are used to assign the tumor cell distributions at these time points as described by Eq. (2). Utilizing the tumor cell growth model either with or without mechanical coupling, a model estimated tumor cell distribution is compared to the observed distribution at the post 1 cycle time point. A map of proliferation, $k(\bar{x})$, and the tumor cell diffusion coefficient, D_0, is iteratively updated until the model/data error is minimized.

3. RESULTS

Figures 2 and 3 show the parameter reconstructions with and without mechanical coupling for the responsive and non-responsive tumors, respectively. Qualitative comparisons of the non-mechanics coupled proliferation rate maps with the mechanics coupled maps for each patient show differences between reconstructed parameter maps. Comparisons between the responsive and non-responsive tumors shows a drastic 10 fold increase towards enhanced cell proliferation with a maximum proliferation rate of ~0.2 and ~2 for the responsive and non-responsive patients, respectively, showing an increase in proliferative capacity of tumor cells for a patient whose clinical outcome results in residual tumor at the conclusion on therapy. Additionally, the mechanics coupled model predictions at the final time point for both patients result in excellent agreement with the observed data as compared to the non-mechanics coupled model in both tumor cell number and spatial distribution. Model predicted final cell numbers for the responsive tumor were 1.58×10^7, and 9.54×10^3 for the non-mechanics and mechanics models, respectively, compared to the observed value of 0 (i.e., no residual tumor burden). Model predicted final cell numbers for the non-responsive tumor were 5.04×10^7, and 3.08×10^7 for the non-mechanics and mechanics models, respectively, compared to 3.08×10^7 for the observed. Comparing the final tumor burden predictions for both models in each tumor (Figure 2h and j and Figure 3h and j, respectively) with their respective observations of final tumor burden (Figure 2f and Figure 3f), the spatial distributions of the mechanics coupled model predictions are seen to exhibit excellent agreement whereas the non-mechanics coupled model are spatially less accurate.

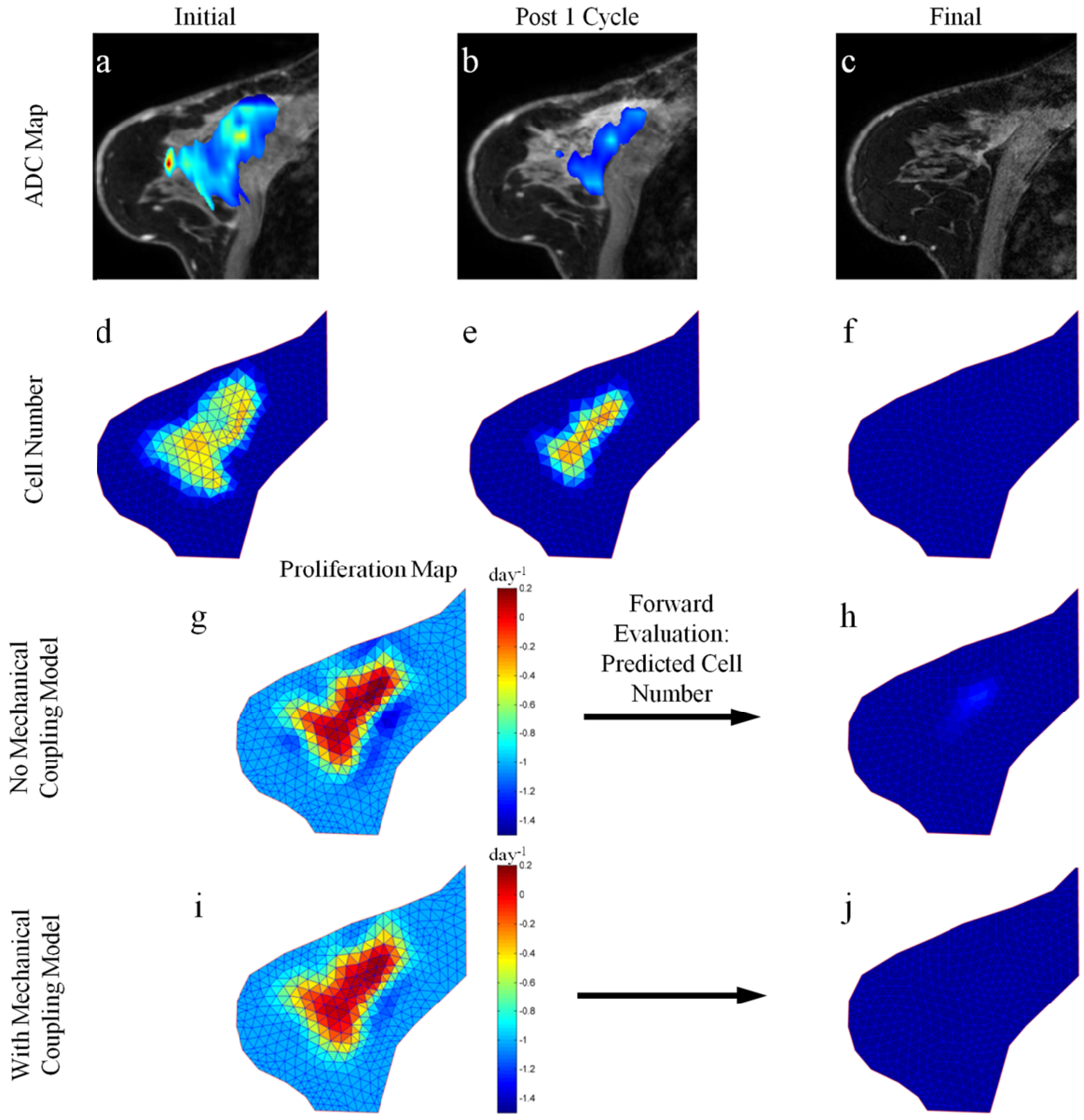

Figure 2. Parameter reconstruction and forward model evaluation for the responsive tumor. ADC maps overlaid on T_1 structural images at initial (a), post one cycle (b), and final (c) time points are converted to cell number distributions (d-f). Parameter optimization using a model without mechanical coupling, as described in Figure 1, is used to reconstruct tumor cell diffusion coefficient and a map of proliferation (g) which is used to predict the final cell number (h). This process is repeated for the model with mechanical coupling (i and j). The predicted final cell number for the model with mechanical coupling (j) is shown to have excellent agreement with the observed final cell number (f).

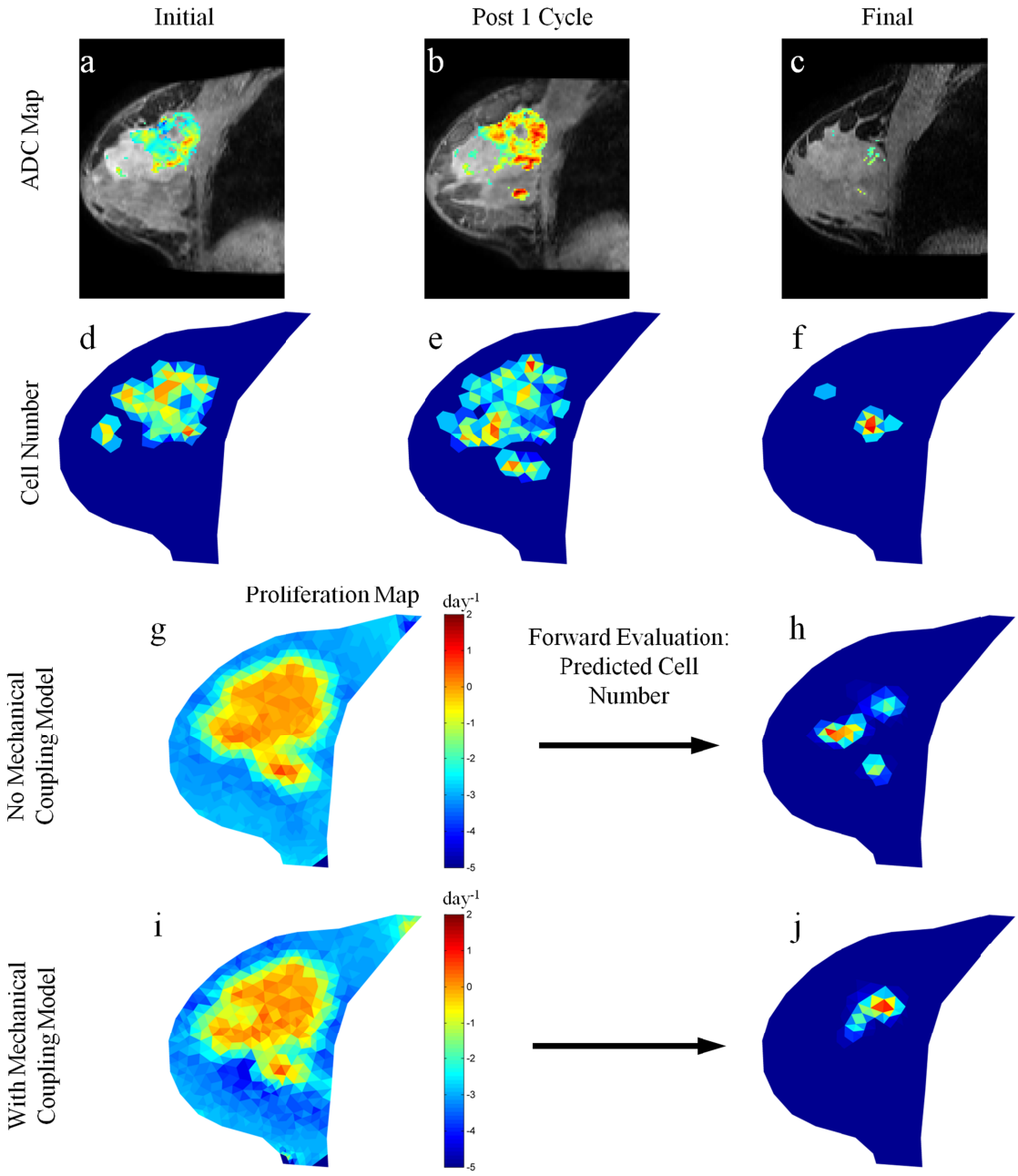

Figure 3. Parameter reconstruction and forward model evaluation for the non-responsive tumor. ADC maps overlaid on T_1 structural images at initial (a), post one cycle (b), and final (c) time points are converted to cell number distributions (d-f). Parameter optimization using a model without mechanical coupling, as described in Figure 1, is used to reconstruct tumor cell diffusion coefficient and a map of proliferation (g) which is used to predict the final cell number (h). This process is repeated for the model with mechanical coupling (i and j). The predicted final cell number for the model with mechanical coupling (j) is shown to have better agreement with the observed final cell number (f).

4. CONCLUSIONS

In this work, we present a mechanically constrained modeling approach to integrate quantitative *in vivo* imaging data into biomathematical models of tumor growth in order to predict eventual response based on early measurements during therapy. The results indicate that the incorporation of mechanics within the biomathematical model impacts the behavior of the model, and thus the parameter reconstructions. Since the therapeutic system is intact, we are able to use the optimized parameters fit between the initial and post one cycle time points to project the model forward in time and compare the model prediction to experimental data for tumor cell number at the final time point. While preliminary, our modeling results provide excellent agreement with clinical observations and suggest that an imaging-based modeling approach to the prediction of tumor response may provide valuable early feedback during the course of neoadjuvant therapy; and our results provide considerable enthusiasm for further studies with more patients. Furthermore, it is very important to note that there is a paucity of efforts in the mathematical modeling literature where *in vivo* clinical measurements are used to generate hypotheses that can actually be tested in individual cancer patients. The framework presented here contributes one such approach to attacking this very important problem.

ACKNOWLEDGEMENTS

We offer our sincerest appreciation to the patients who selflessly volunteered to participate in this study. We thank the National Institutes of Health for funding through NCI 1U01CA142565, R25CA092043, NCI 1P50 098131 and the Vanderbilt-Ingram Cancer Center Support Grant (NIH P30 CA68485). We thank the Kleberg Foundation for generous support of the imaging program at our Institution.

REFERENCES

[1] Garg, I. and Miga, M. I., "Preliminary investigation of the inhibitory effects of mechanical stress in tumor growth," Proc. SPIE 6918, Medical Imaging 2008: Visualization, Image-guided Procedures, and Modeling (2008).

[2] Hogea, C., Davatzikos, C., and Biros, G., "An image-driven parameter estimation problem for a reaction-diffusion glioma growth model with mass effects," Journal of Mathematical Biology 56(6), 793-825 (2008).

[3] Szeto, M. D., Chakraborty, G., Hadley, J., Rockne, R., Muzi, M., Alvord, E. C., Jr., Krohn, K. A., Spence, A. M., and Swanson, K. R., "Quantitative metrics of net proliferation and invasion link biological aggressiveness assessed by MRI with hypoxia assessed by FMISO-PET in newly diagnosed glioblastomas," Cancer Res 69(10), 4502-4509 (2009).

[4] Ellingson, B. M., LaViolette, P. S., Rand, S. D., Malkin, M. G., Connelly, J. M., Mueller, W. M., Prost, R. W., and Schmainda, K. M., "Spatially quantifying microscopic tumor invasion and proliferation using a voxel-wise solution to a glioma growth model and serial diffusion MRI," Magn Reson Med. 65(4), 1131-1143 (2011).

[5] Ratain, M. J., and Eckhardt, S. G., "Phase II studies of modern drugs directed against new targets: if you are fazed, too, then resist RECIST," J Clin Oncol 22(22), 4442-4445 (2004).

[6] Tuma, R.S., "Sometimes size doesn't matter: reevaluating RECIST and tumor response rate endpoints," J Natl Cancer Inst 98(18), 1272-1274 (2006).

[7] Li, X., Dawant, B. M., Welch, E. B., Chakravarthy, A. B., Freehardt, D., Mayer, I., Kelley, M., Meszoely, I., Gore, J. C., and Yankeelov, T. E., "A nonrigid registration algorithm for longitudinal breast MR images and the analysis of breast tumor response," Magn Reson Imaging 27(9), 1258-1270 (2009).

[8] Li, X., Dawant, B. M., Welch, E. B., Chakravarthy, A. B., Xu, L., Mayer, I., Kelley, M., Meszoely, I., Means-Powell, J., Gore, J. C., and Yankeelov, T. E., "Validation of an algorithm for the nonrigid registration of longitudinal breast MR images using realistic phantoms," Med Phys 37(6), 2541-2552 (2010).

[9] Anderson, A. W., Xie, J., Pizzonia, J., Bronen, R. A., Spencer, D. D., and Gore, J. C., "Effects of cell volume fraction changes on apparent diffusion in human cells," Magn Reson Imaging 18(6), 689-695 (2000).

[10] Martin, I., Dozin, B., Quarto, R., Cancedda, R. and Beltrame, F. "Computer-based technique for cell aggregation analysis and cell aggregation in in vitro chondrogenesis," Cytometry 28, 141-146 (1997).